

Controls on the deposition of extremely large post-earthquake debris flows in Wenchuan

Erin Harvey, Tristram Hales, Daniel Hobley, Alexander Horton, Jie Liu, and Xuanmei Fan

1. Introduction

- Post-earthquake debris flows pose significant hazards to local communities and facilitate the transport of sediment from hillslopes into channels following an earthquake.
- In 2019, at least 13 debris flows transported sediment across four stream orders before depositing in the Min Jiang River. These debris flows were highly fluidised, extremely large and therefore important from a sediment transport and hazard perspective. However, the mechanisms controlling these debris flows are poorly understood.
- **We compare the grain size distributions (GSDs) deposited by two debris flows with similar triggering conditions and initiation mechanisms to better understand why they developed into debris flows with very different runout lengths. We aim to better understand how the depositional mechanisms relating to grain size differ between the two flows.**

2. Study Sites & Methods

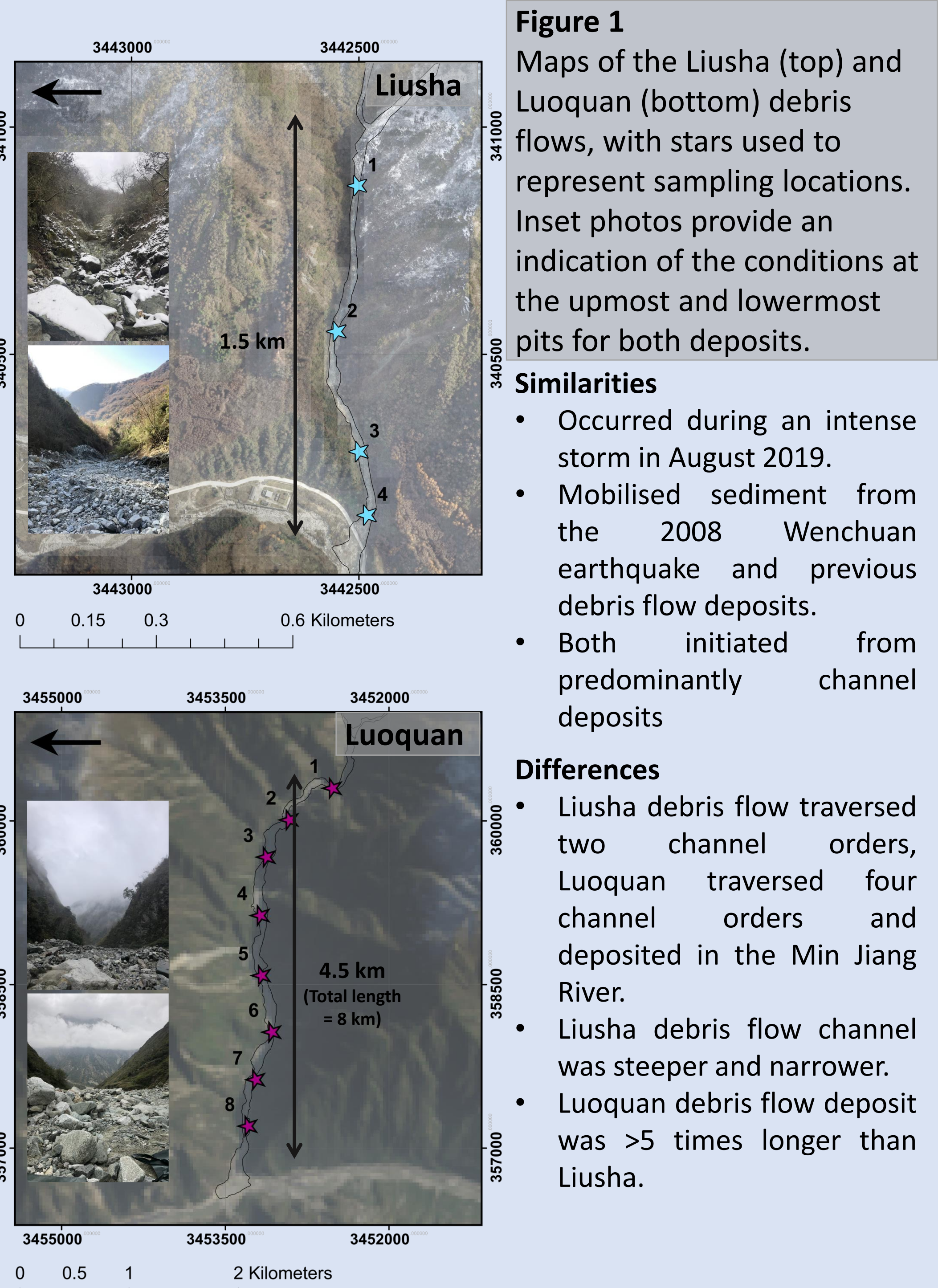


Figure 1 Maps of the Liusha (top) and Luoquan (bottom) debris flows, with stars used to represent sampling locations. Inset photos provide an indication of the conditions at the upmost and lowermost pits for both deposits.

- Similarities**
- Occurred during an intense storm in August 2019.
 - Mobilised sediment from the 2008 Wenchuan earthquake and previous debris flow deposits.
 - Both initiated from predominantly channel deposits

- Differences**
- Liusha debris flow traversed two channel orders, Luoquan traversed four channel orders and deposited in the Min Jiang River.
 - Liusha debris flow channel was steeper and narrower.
 - Luoquan debris flow deposit was >5 times longer than Liusha.

GSDs
GSDs were collected using sieving and photos along transects (Figure 1).

GSD integrals
GSD integrals by integrating the curve of a normalised grain size and fraction coarser than plot (Figure 2), with increasing integrals corresponding to coarser GSDs.

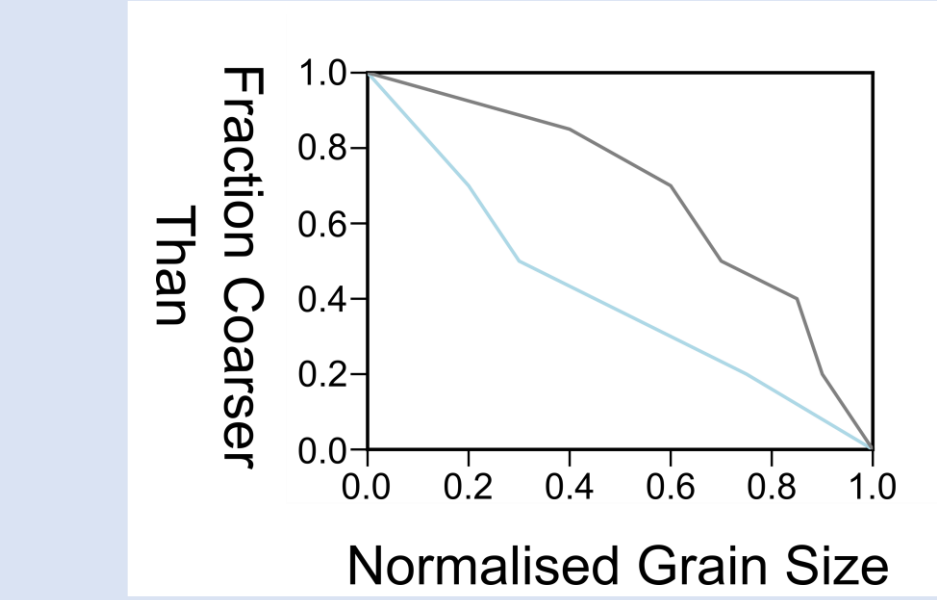


Figure 2 (above) An example of the plot used to determine GSD integrals for each distribution.

Figure 3 (right) We used sieving and photos to determine subsurface and surface GSDs for the two debris flow deposits.



3. Vertical GSDs

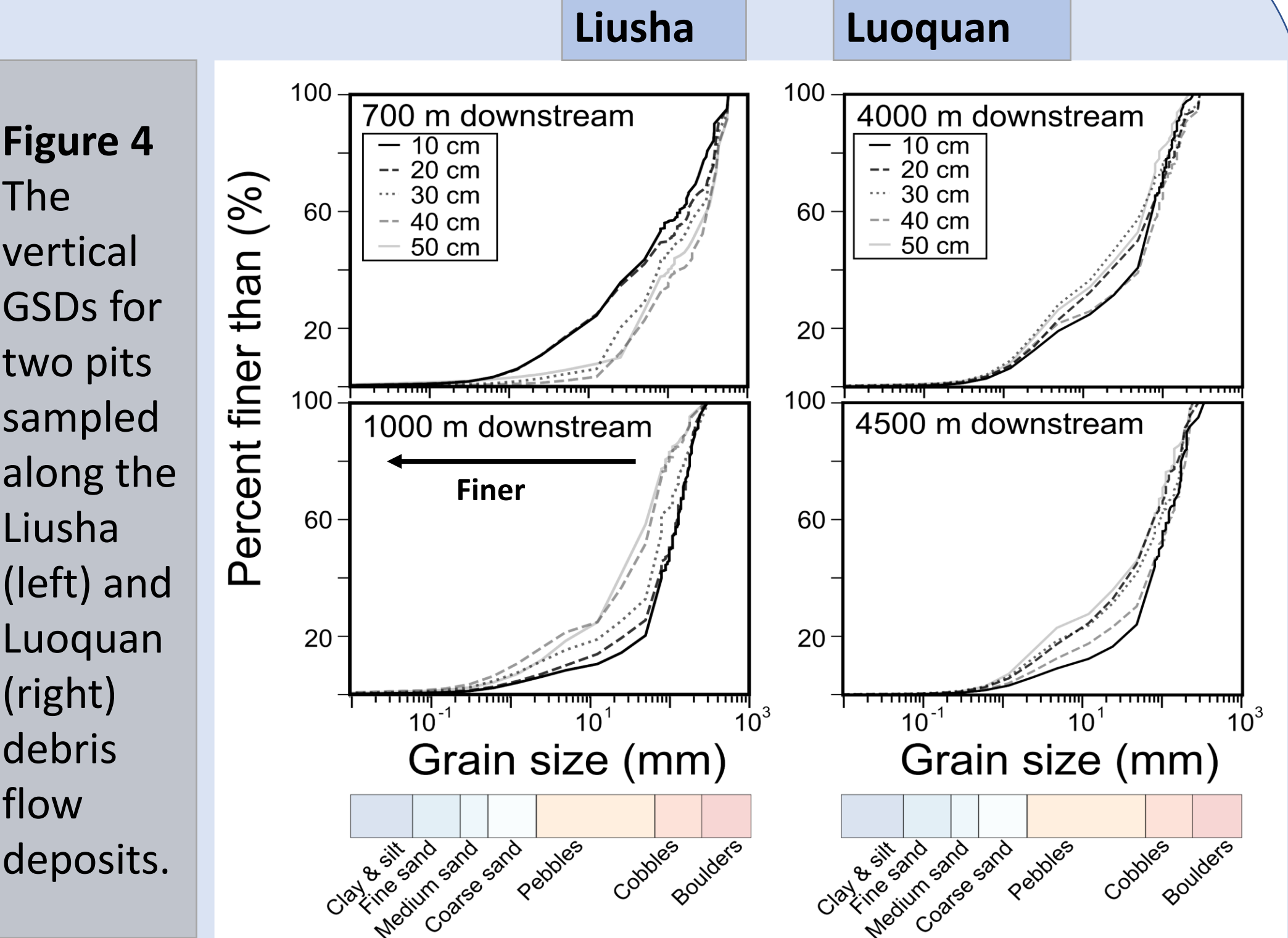
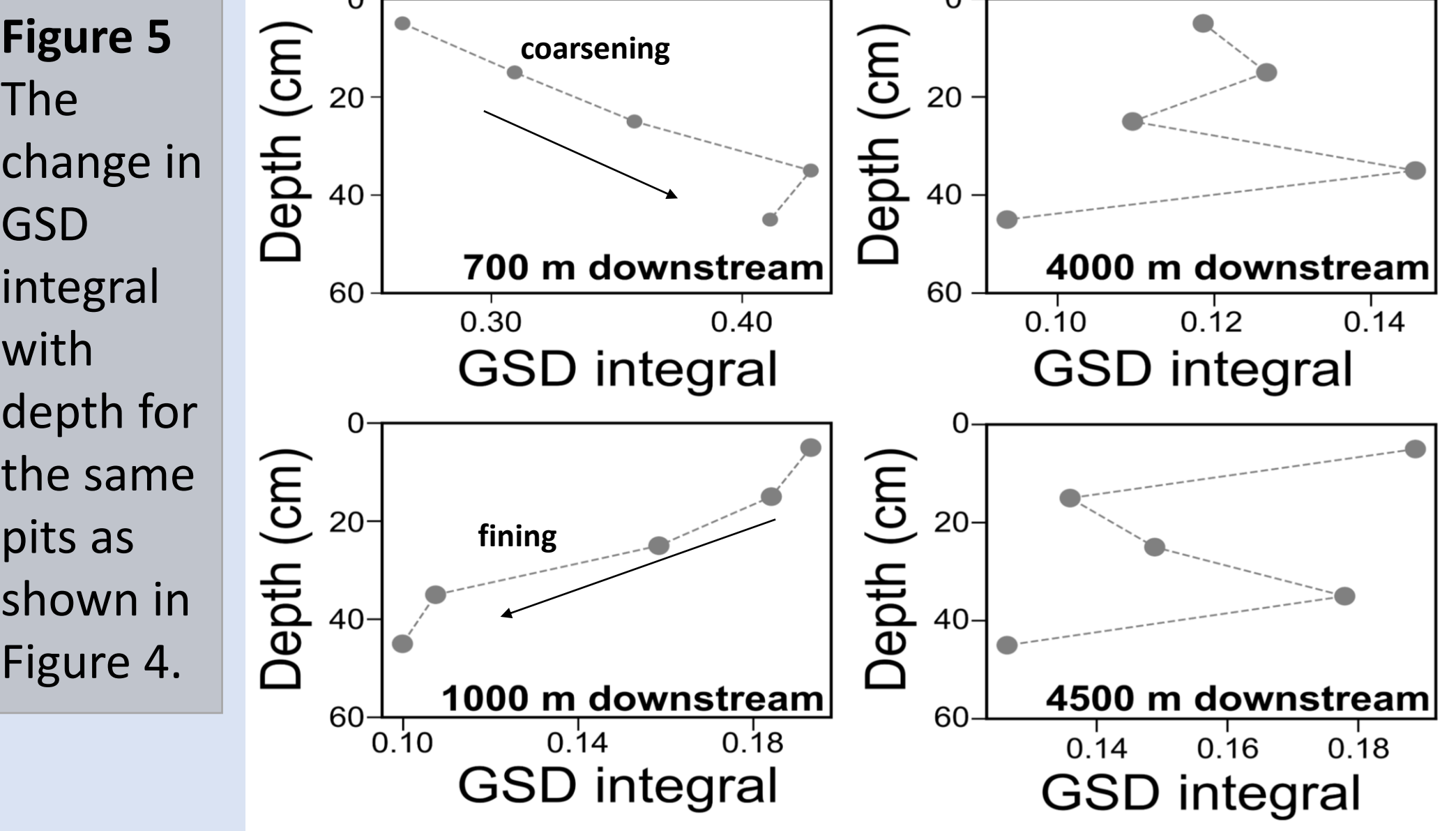


Figure 4 The vertical GSDs for two pits sampled along the Liusha (left) and Luoquan (right) debris flow deposits.



We observed both **normally and inversely graded deposits in Liusha**, with a coarsening with depth at 700 m downstream (normal grading) and a fining with depth at 1000 m downstream (inverse grading). In **Luoquan**, we observed **no relationship for the vertical GSDs** in the deposit. The absence of a relationship suggests segregation by grain size may not have taken place during the flow due to highly viscous flows or high pore fluid pressures. Thus, supporting our observation of a highly fluid, large debris flow.

6. Conclusions

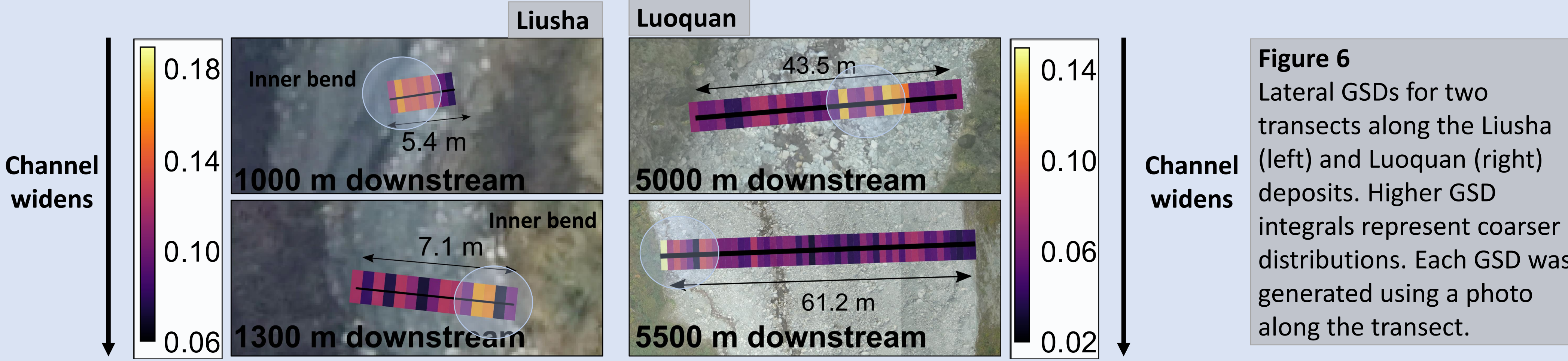
The Liusha and Luoquan debris flows deposited similar GSDs in terms of grain size width and maximum grain size, however the vertical, lateral and longitudinal distributions of the deposited grains differed greatly.

These differences may be attributed to the different deposition mechanisms within the flow, for example evidence of segregation in Liusha suggests that a velocity gradient may have been present in the flow and the shouldering of coarse deposits may have resulted in frictional deposition.

Whereas in Luoquan size segregation was not observed.

In Luoquan, channel width and curvature appeared to correspond with changes in the grain size fractions deposited between 4000 m and 6500 m downstream, suggesting topography may in part control the deposition of extremely, large, fluidised debris flows.

4. Lateral GSDs



We found that the **coarsest GSDs** corresponded to the **edge and inner bend** of channels in **Liusha**. We also found a **decrease** in the proportion of the channel with **large (>0.14) GSD integrals** with **increasing channel width**. The deposition of coarse grains along the channel edge may be explained by the formation of **unpaired levees** through vertical and lateral segregation or the **lower flow velocities** on the inner bend of the channel encouraging the deposition of larger grains.

In Luoquan, the **lateral deposition of coarse grains** was **more variable**, with high GSD integrals both in the channel and along the edge of channels. However, similar to in Liusha, we noticed that when the **channel widened**, as shown above, there was a **decrease** in the proportion of **high GSD integrals (>0.10)**. The relationships with channel width suggest channel topography may be an important control in the deposition of large debris flows.

5. Longitudinal GSDs

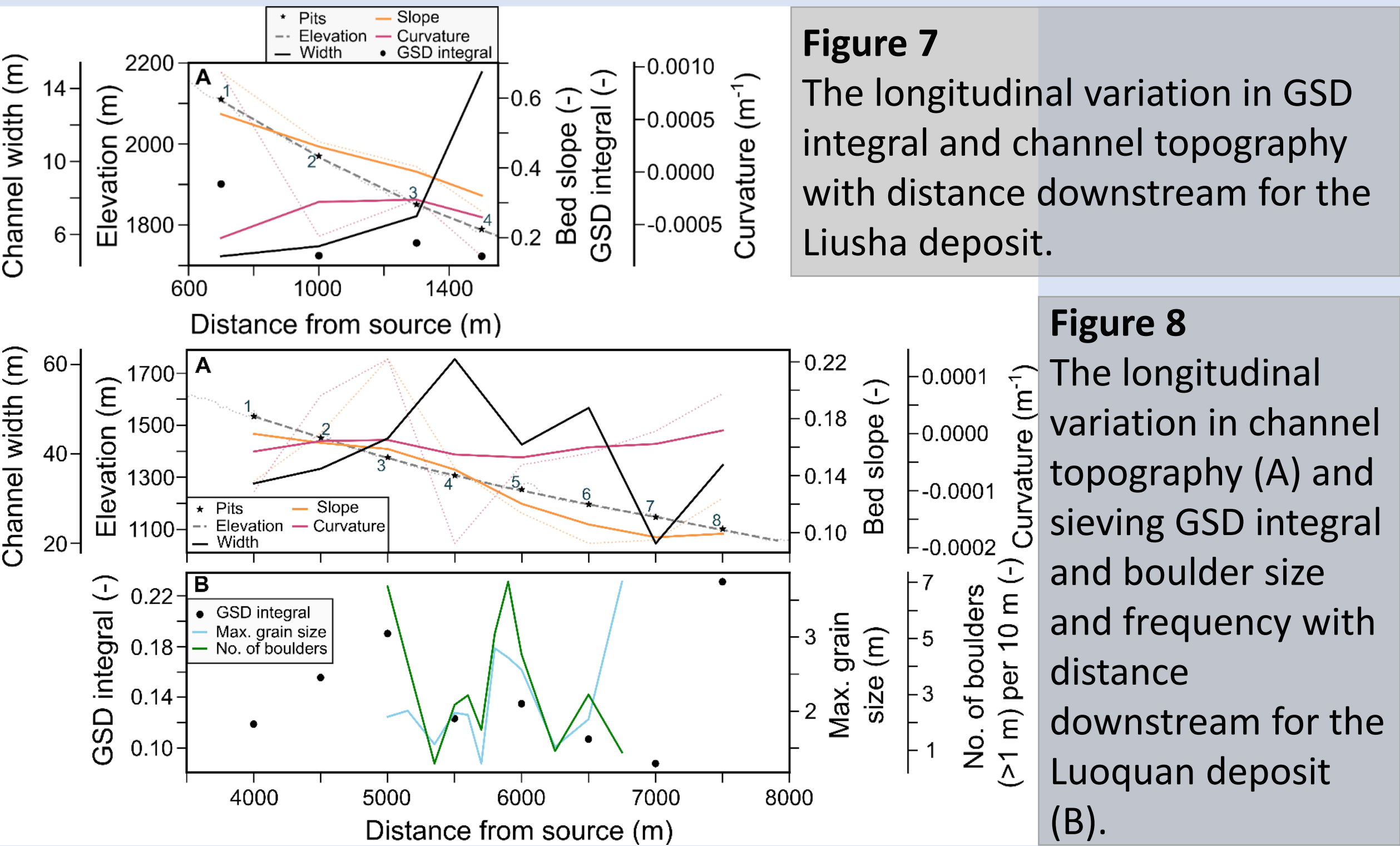


Figure 7 The longitudinal variation in GSD integral and channel topography with distance downstream for the Liusha deposit.

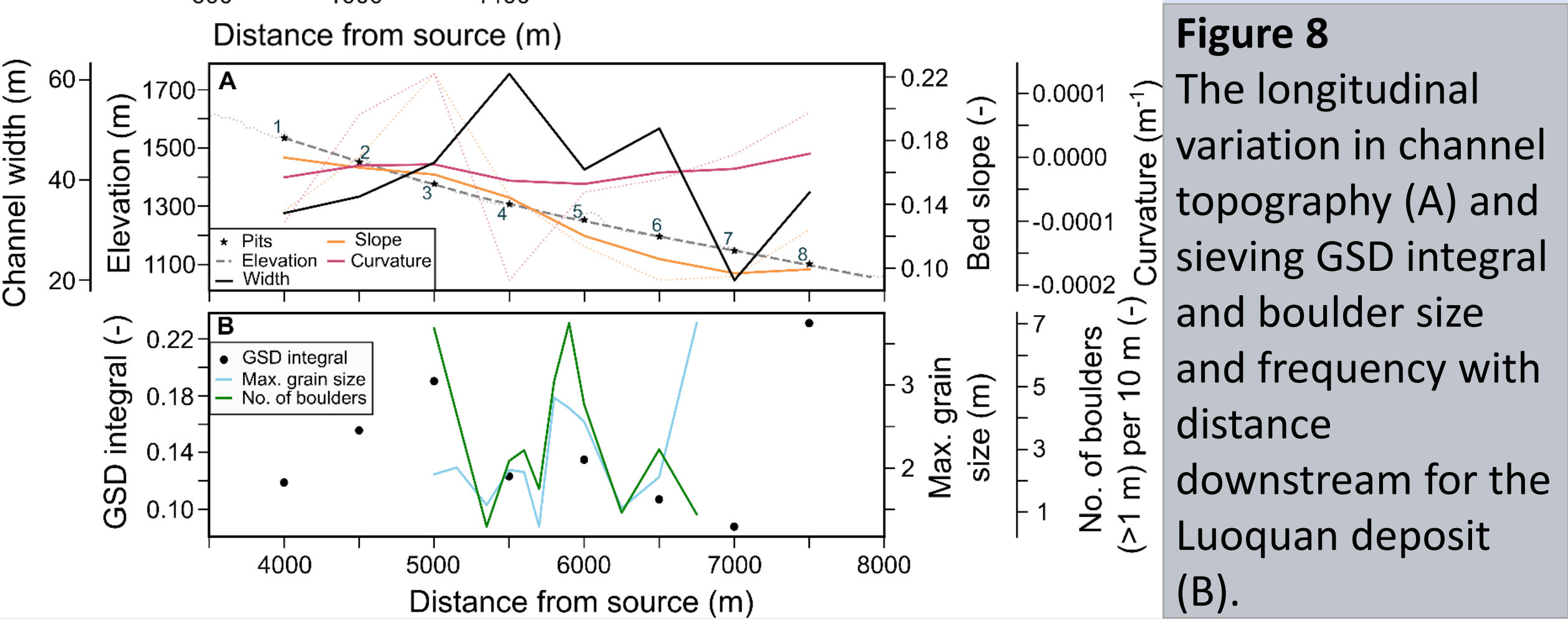


Figure 8 The longitudinal variation in channel topography (A) and sieving GSD integral and boulder size and frequency with distance downstream for the Luoquan deposit (B).

In Liusha, there was a general **downstream decrease** in the **GSD integral**. Topographically there was an increase in channel width and a decrease in channel slope with distance downstream.

In Luoquan the channel slopes are more variable with distance downstream and shallower in comparison to Liusha. Channel width also changes with distance downstream. Increases in **channel width** corresponded with a **decrease in the size and frequency of boulders** deposited. The **GSD integrals varied downstream**, with an initial increase with increasing curvature to 5000 m downstream followed by a sharp decrease, where we also find a decrease in curvature and an increase in channel width.